*R*esearch in
*A*stronomy and
*A*strophysics

TeV cosmic-ray proton and helium spectra in the myriad model II *

Wei Liu[1,2], Pierre Salati[3], Xuelei Chen[1,4]

[1] National Astronomical Observatories, Chinese Academy of Science, Beijing 100012, China
[2] University of Chinese Academy of Sciences, Beijing 100049, China; *weiliu@bao.ac.cn*
[3] LAPTh, Université de Savoie, CNRS, BP 110, 74941 Annecy-le-Vieux, France;
   salati@lapth.cnrs.fr
[4] Center of High Energy Physics, Peking University, Beijing 100871, China;
   xuelei@cosmology.bao.ac.cn

Abstract Recent observations show that the spectra of cosmic ray nuclei start to harden above $\sim 10^2$ GeV, which contradicts the conventional steady-state cosmic ray model. We had suggested that this anomaly is due to the propagation effect of cosmic rays released from local young cosmic ray sources; the total flux of cosmic rays should be computed with the Myriad Model, where a contribution from sources in the local catalog is added to the background. However, although the hardening could be elegantly explained in this model, the model parameters obtained from the fit are skewed toward a region with fast diffusion and a low supernova rate in the Galaxy, in disagreement with other observations. We further explore this model in order to set up a concordant picture. Two possible improvements related to cosmic ray sources are considered. First, instead of the usual axisymmetric disk model, we examine a spiral model for the source distribution. Second, for nearby and young sources which are necessary to explain the hardening, we allow for an energy-dependent escape. We find that a major improvement comes from incorporating an energy-dependent escape time for local sources, and with both modifications not only are the cosmic ray proton and helium anomalies resolved, but also the parameters attain values in a reasonable range compatible with other analyses.

Key words: catalogs — cosmic rays — pulsars: general — galaxies: spiral

1 INTRODUCTION

It is generally accepted that most high energy cosmic ray particles are accelerated in supernova shocks, and form simple power law spectra $q \propto \mathcal{R}^{-\alpha}$, where $\mathcal{R} \equiv p/Ze$ denotes the rigidity of a particle (Axford et al. 1977; Krymskii 1977; Bell 1978; Blandford & Ostriker 1978). After being injected into interstellar space, the particles are frequently scattered by magnetic irregularities in the Galaxy. This could be described approximately as a diffusion process with spatial diffusion

coefficient $K \propto \mathcal{R}^\delta$ (Berezinskii et al. 1990; Maurin et al. 2002b). The diffusion volume is called the magnetic halo. Once these cosmic rays reach a steady state in the halo, the observed cosmic-ray fluxes are described in a large energy range by $\Phi \propto q/K$; i.e. the spectrum scales with energy as a single power law $E^{-(\alpha+\delta)}$, where both α and δ are constant.

Recently, the observations by the CREAM (Ahn et al. 2010; Yoon et al. 2011) and PAMELA (Adriani et al. 2011) experiments indicated a hardening in the spectra of cosmic ray nuclei above 250 GeV/nucleon. This extends to TeV energies, though the low energy spectrum measured by the AMS-02 experiment (AMS-02 2013; Consolandi & on Behalf of the AMS-02 Collaboration 2014) differs somewhat from the result of PAMELA, and for the result from AMS-02 the hardening is not as significant as the one from PAMELA. This problem will be further checked by other experiments, e.g. the ASγ experiment (Tibet Asγ Collaboration et al. 2011; Amenomori et al. 2011) in Yangbajing, Tibet.

A number of different models have been proposed to explain the PAMELA and CREAM anomaly. Most of these focus on the change of energy dependence of either the injection spectrum $q(E)$ (Biermann et al. 2010; Ohira & Ioka 2011; Yuan et al. 2011; Malkov et al. 2012) or the diffusion coefficient $K(E)$ (Ave et al. 2009; Blasi et al. 2012). A local variation in K proposed by Tomassetti (2012) could induce a similar effect. In addition, Blasi & Amato (2012) invoke an unusually strong spallation of species on Galactic gas, but this has been criticized by Vladimirov et al. (2012). More recently, Thoudam & Hörandel (2013a) considered the diffusive re-acceleration effect, through which the injected energy spectrum can be modified at low energies.

Bernard et al. (2013) proposed that the excess of cosmic-ray nuclei at high energy comes from a particular configuration of local sources. To compute the flux of the primary cosmic ray nuclei, instead of the regular steady-state transport model, the myriad-source model (Higdon & Lingenfelter 2003) is employed. In this model, the cosmic ray flux is computed in a time-dependent transport framework. For young and nearby sources, a detailed and complete catalog was constructed using current survey data, and its contribution was calculated separately. New values of the transport parameters were obtained, which fit the proton and helium excess as well as the B/C ratio.

However, although this model could reproduce the observed spectra, it is not completely satisfactory. The best fit model parameters indicate there is either a thin magnetic halo or a low supernova rate in the Galaxy, but these disagree with other observations, for example γ-ray and synchrotron emissions (Strong et al. 2010; Bringmann et al. 2012; Di Bernardo et al. 2013). All these results favor a medium size magnetic halo, but for such a halo, e.g. $L \sim 4$ kpc, a low supernova explosion rate is required, at nearly the lower limit imposed by observations (Diehl et al. 2006). It might be that the contribution from the background sources was overestimated. Another possible problem is that the process used to explain how cosmic ray particles escape from local supernova remnants (SNRs) was incorrectly modeled.

In this paper we consider two possible improvements to this model. In previous studies (Bernard et al. 2013), we have assumed that the background sources are distributed axisymmetrically in the Galactic disk. In fact, the sources, i.e. SNRs are likely distributed along the spiral arms, and to our knowledge the solar system is located between two of them. This difference in the source distribution may affect the result. Moreover, we shall also take the macroscopic size of the local sources and the energy-dependent escape time into account (Thoudam & Hörandel 2012, 2013b). We shall investigate if the fitting to cosmic ray data can be improved, especially with a higher supernova explosion rate. We also incorporate more recent and more precise AMS-02 data (AMS-02 2013; Consolandi & on Behalf of the AMS-02 Collaboration 2014) into our analysis.

The paper is arranged as follows: Sections 2 and 3 introduce the cosmic-ray propagation model and sources respectively. The results are shown in Section 4. Finally, we give our discussion and conclusions in Section 5.

2 COSMIC RAY PROPAGATION MODEL

The galactic supernova explosions which inject cosmic ray particles into interstellar space can be regarded as a stationary random process. During the average lifetime of the cosmic ray particles, the number of supernova explosions is large; as a result a nearly steady average flux is established. However, for short time scales (still large compared with human history) and on scales relevant for observation (solar system), statistical fluctuations can still be large (Bernard et al. 2012), and the contribution of young and nearby sources could result in significant deviation from the average. This could be a possible reason for the observed excess at high energies. To address this possibility, we separate the cosmic ray sources into two components: the remote or aged SNRs which produce a nearly steady background, and the recent and nearby sources, which could produce a local deviation in the spectrum. We model the local population by using information collected from current SNR surveys. Similar ideas were also explored by Erlykin & Wolfendale (2012) and Thoudam & Hörandel (2012); we expanded this local population to the whole energy range from tens of GeV up to a few PeV (Bernard et al. 2013). The key idea here is that nearby sources are used to explain the spectral hardening at high energies, whereas the bulk of the remote and old sources account for fluxes below 250 GeV/nuc. The more energetic particles spend less time in the magnetic halo, making their contribution from local and recent SNRs more important at high energies.

We are mainly interested in the high energy distribution, so diffusive re-acceleration is neglected, as it mostly acts on low energy particles. If we define $\psi \equiv \mathrm{d}n/\mathrm{d}T$ as the number density per unit volume unit kinetic energy of a given cosmic ray species, the diffusion equation is

$$\frac{\partial \psi}{\partial t} + \partial_z(V_c \psi) - K(E)\Delta\psi + 2h\delta(z)\,\Gamma_{\mathrm{sp}}\psi = Q_{\mathrm{acc}}\,, \tag{1}$$

where V_c is the convective velocity at which cosmic ray particles are blown away from the galactic disk by the stellar wind. The spatial diffusion coefficient is $K(E) = \kappa_0 \beta \mathcal{R}^\delta$, where κ_0 is a normalization constant and $\beta = v/c$ denotes the particle velocity v in units of the speed of light c. Generally, the diffusion coefficients form a tensor and are position-dependent, but here for simplicity we assume diffusion to be uniform and isotropic within the magnetic halo. The total cosmic ray flux is $\Phi = v\psi/(4\pi)$. The magnetic halo inside which cosmic ray particles diffuse is assumed to be a flat cylinder, whose thickness $2L$ is an unknown parameter to be determined from fitting to the data. A uniform Galactic disk is located in the middle of the halo and its thickness is about $200\,\mathrm{pc}$. The radius of the magnetic halo is usually set to be equal to the Galactic radius $R = 20\,\mathrm{kpc}$. Beyond the magnetic halo, the magnetic field drops rapidly, and the cosmic ray particles are no longer confined. Customarily, at the boundary the free escape condition is assumed. The last term on the left-hand side of Equation (1) is the spallation term, with the collision rate Γ given by

$$\Gamma_{\mathrm{sp}} = v(\sigma_{\mathrm{pH}}n_{\mathrm{H}} + \sigma_{\mathrm{pHe}}n_{\mathrm{He}})\,, \tag{2}$$

in the case of cosmic ray protons. The average densities of hydrogen and helium, n_{H} and n_{He}, in the disk are 0.9 and $0.1\,\mathrm{cm}^{-3}$ respectively. The cross section σ_{pH} is given in Nakamura & Particle Data Group (2010), and σ_{pHe} is assumed to be $4^{2.2/3}\sigma_{\mathrm{pH}}$ (Norbury & Townsend 2007). For helium cross sections the same scaling factor is adopted.

The sources are assumed to be point-like

$$Q_{\mathrm{acc}}(\boldsymbol{x}_S, t_S) = \sum_{i \in \mathcal{P}} q_i\,\delta^3(\boldsymbol{x}_S - \boldsymbol{x}_i)\delta(t_S - t_i)\,, \tag{3}$$

where q_i, $\boldsymbol{x}_i$ and t_i denote the injection amount, position and time for the ith explosion respectively. For simplicity, we assume q_i to be identical for all the sources and given by

$$q_i^j(p) = q_j^0 \left(\frac{p}{1\,\mathrm{GeV/nuc}}\right)^{-\alpha_j}\,, \tag{4}$$

for the jth element. The parameters q_j^0 and α_j for protons and helium are determined from parameter fitting. The solution of the transport equation (1) can be written in terms of the Green function as

$$\psi(\boldsymbol{x}, t) = \int_{-\infty}^{t} \mathrm{d}t_S \int_{MH} \mathrm{d}^3\boldsymbol{x}_S \, \mathcal{G}_p(\boldsymbol{x}, t \leftarrow \boldsymbol{x}_S, t_S) \, Q_{\mathrm{acc}}(\boldsymbol{x}_S, t_S) \,. \tag{5}$$

The diffusion equation can be solved by numerical integration using the code GALPROP (Strong & Moskalenko 1998; Strong et al. 2007) and its succeeding code DRAGON (Evoli et al. 2008; Di Bernardo et al. 2010) package. Here we consider another approach, the semianalytical model (Maurin et al. 2001, 2002a,b). As the diffusion equation is linear, we can write the cosmic ray flux as

$$\Phi = \Phi_{\mathrm{cat}} + \Phi_{\mathrm{ext}} \,, \tag{6}$$

where Φ_{cat} is the contribution of the nearby and recent sources given in the catalog, and Φ_{ext} is the flux from background sources, which can be approximated by its time average $\bar{\Phi}_{\mathrm{ext}}$ (Bernard et al. 2012). The nearby recent supernova explosions can produce fluctuations in cosmic ray fluxes. With data from current surveys, a catalog of nearby SNRs can be constructed. However, SNRs have limited lifetimes, and faint sources may still be missed. Pulsars are usually regarded as relics of supernova explosions, and are good tracers of aged SNRs. They can be added to known SNRs as a complementary catalog. A list of cosmic ray sources derived from the Green catalog (Green 2009) and ATNF pulsar database (Manchester et al. 2005) was presented in Bernard et al. (2013), with the millisecond pulsars associated with known SNRs removed to avoid double counting. In this list, the radial distance extends up to 2 kpc from the Sun, and the upper limit on the age is set to 30 000 years, within which there are 30 sources in total. This is consistent with a supernova explosion rate of 3 per century (Bernard et al. 2012), which could be a local fluctuation on the high side since Earth is located between two nearby spiral arms.

3 IMPROVEMENTS IN THE SOURCE MODEL

3.1 Spiral Distribution of Cosmic Ray Sources

Previously, the cosmic ray source distribution was usually assumed to be azimuthally symmetric in the Galaxy. This is appropriate when the diffusion distance is much larger than the characteristic scale between spiral arms, but when evaluating cosmic ray fluxes at high energies where local sources could play a dominant role, the specific position of the solar system and its local environment may be important.

The Milky Way Galaxy is a typical spiral galaxy, and the high density gas inside spiral arms triggers rapid star formation, so cosmic ray sources are also highly correlated with the spiral arms. The spiral distribution of sources has been considered in some recent studies (Shaviv 2003, 2002; Shaviv et al. 2009; Effenberger et al. 2012; Blasi & Amato 2012). There are still some uncertainties in the structure and pattern speed of the spiral arms, owing to our position in the Galaxy. While the outer part of the Milky Way seems to have four arms, for the inner part the number of arms is still being debated. The different measurements for the spiral structure and number of spiral arms are reviewed in Vallee (1995); Vallée (2002) and Elmegreen (1998). In this paper, we adopt the spiral model given in Faucher-Giguère & Kaspi (2006). Similar models were also adopted by Blasi & Amato (2012) and Gaggero et al. (2013). In this model, the whole Galaxy is assumed to be made of four major arms spiraling outward from the Galactic center, as featured in Figure 1. The locus of the ith arm is on a logarithmic spiral defined by the relation $\theta(r) = k^i \ln(r/r_0^i) + \theta_0^i$, where the parameters k^i, r_0^i and θ_0^i are borrowed from Faucher-Giguère & Kaspi (2006). For the radial distribution of sources, the parameterization of Yusifov & Küçük (2004) is applied,

$$\rho(r) = \left(\frac{r + R_1}{R_\odot + R_1} \right)^a \exp\left[-b \left(\frac{r - R_\odot}{R_\odot + R_1} \right) \right] \,, \tag{7}$$
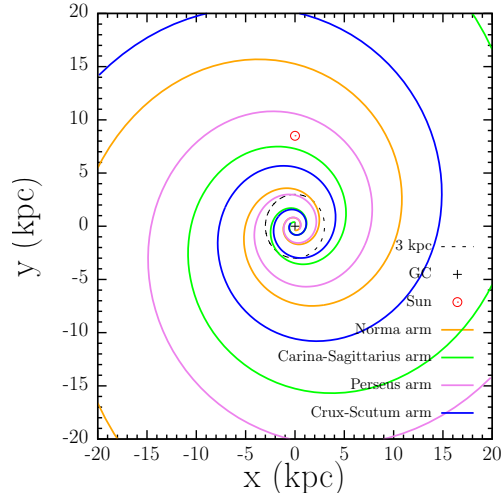
Fig. 1 The Galaxy is assumed to have four spiral arms, with the Sun lying between the Carina–Sagittarius and Perseus arms, about 8.5 kpc away from the Galactic center (Faucher-Giguère & Kaspi 2006).

with the best-fit values $a = 1.64, b = 4.01$ and $R_1 = 0.55$ kpc. The solar system is located between the Carina-Sagittarius and Perseus spiral arms, with $\boldsymbol{R}_\odot = \{0, 8.5, 0\}$ in units of kpc. Along the spiral arm, there is a spread in the radial coordinate that follows a normal distribution

$$f_i = \frac{1}{\sqrt{2\pi}\sigma} \exp\left(-\frac{(r - r_i)^2}{2\sigma^2}\right), \qquad i \in [1, 2, 3, 4], \tag{8}$$

where r_i is the inverse function of the locus of the ith spiral arm and the standard deviation σ is taken to be $0.07\, r_i$. The vertical distribution from the Galactic plane is a decreasing exponential function with mean $z_0 = 100$ pc. Different measurements have been used to determine the pattern speed. Here we take $\Omega_\odot - \Omega_{p,\max}$ to be $7.7\,\mathrm{km\,s^{-1}\,kpc^{-1}}$(Shaviv 2003). Faucher-Giguère & Kaspi (2006) also modified their model in the inner 3 kpc of the Galaxy to account for the more axisymmetric core, but for our calculation at the solar position this makes little difference, so we simply use the spirals for calculation.

3.2 Energy-Dependent Escape

In the usual treatment, the inherent size and duration of the source are neglected; all the cosmic ray particles are assumed to be instantly released into interstellar space once a supernova explodes. This approximation is reasonable when we are considering scales much larger than the size and duration of sources. However, as we noted above, at high energies the role of recent nearby sources may be important, and the observed cosmic ray anomaly may be a local fluctuation; then, these neglected factors may also need to be taken into account (Thoudam & Hörandel 2012, 2013b).

According to the diffusive shock acceleration theory, charged particles are accelerated during their repeated crossings of the shock front. They are confined within the supernova shock by magnetic turbulence until their upstream diffusion length l_d is larger than the shock radius, which is growing with time. The diffusion length is given by $l_d = D_s/u_s$, where D_s is the diffusion coefficient in the upstream region and u_s is the shock velocity. In the Bohm limit, the diffusion coefficient D_s in the upstream region increases linearly with energy E, $D_s(E) \propto E$. Thus in general, the

most energetic particles escape from the acceleration region earlier. However, the details of how the cosmic rays escape from the source are still not well understood.

The escape time is generally parameterized as

$$t_{esc}(\mathcal{R}) = t_{sed} \left(\frac{\mathcal{R}}{\mathcal{R}_{max}} \right)^{-1/\gamma},$$ (9)

where $t_{sed} = 500$ yr is the onset time of the Sedov phase, and the maximum rigidity $\mathcal{R}_{max} = 1$ PV. The escape index γ is a positive constant that determines the span of the escape time. When $\gamma \gg 1$, the escape is very close to an instantaneous injection into space. Usually this parameter lies between 1 and 3. When the shock is too weak to accelerate particles and the level of turbulence in the upstream region can no longer hold them, the rest of the cosmic ray particles are released all at once. This is assumed to happen in 10^5 years, so the cosmic ray escape time is taken to be

$$T_{esc}(E) = \min(t_{esc}, 10^5 \text{ yr}).$$ (10)

Along with shock expansion, the shock radius increases according to the Sedov relation

$$R_{esc}(E) = 2.5 \, u_0 \, t_{sed} \left\{ \left(\frac{T_{esc}}{t_{sed}} \right)^{0.4} - 0.6 \right\},$$ (11)

where $u_0 = 10^7$ m s^{-1} represents the initial velocity of the shock at time t_{sed}. If cosmic rays are assumed to escape from the surface, which is supposed to be spherically symmetric, the source term in Equation (1) turns out to be

$$Q(E, t, r) = \frac{q(E)}{A_{esc}} \, \delta(t - T_{esc}) \, \delta(r - R_{esc}),$$ (12)

where $A_{esc} = 4\pi R_{esc}^2$ is the surface area of the SNR at the escape time T_{esc}, and r denotes the distance to the center of the SNR.

4 RESULTS

We now try to find the best-fit parameter values by comparing the model prediction on proton and helium spectra with the data from the AMS-02 (AMS-02 2013) and CREAM (Ahn et al. 2010) experiments. We perform the fit in the energy range from 50 GeV/nuc to 100 TeV/nuc, where the solar modulation can be safely neglected. The quality of the fit to the data is analyzed quantitatively by χ^2/d.o.f., with the proton and helium data, $\chi^2 = \chi_p^2 + \chi_{He}^2$. Our cosmic ray propagation model is defined by the transport parameters K_0, δ, V_c and L. All of these are restricted within a range that is consistent with the secondary-to-primary B/C measurements (Maurin et al. 2001). In addition, we have parameters which specify the source properties, including q_p^0, q_{He}^0, α_p and α_{He} in Equation (4), and the average supernova explosion rate ν. Finally, for the energy-dependent escape model, one more parameter, the escape index γ also needs to be included. The parameters and goodness of fit for the models considered in this paper are listed in Table 1.

In our previous work (Bernard et al. 2013), we studied several configurations, but the supernova explosion rates were close to the lower observational limit, unless L is extremely small. In this paper, we fix the propagation parameters to the MED configuration of Donato et al. (2004); Bernard et al. (2013), where the vertical boundary of halo L has the plausible value of 4 kpc, and also best fits the B/C data (Maurin et al. 2001). We perform a scan over supernova explosion rate, which is required to be larger than 0.8 century^{-1}. Once the transport parameters and the explosion rate are fixed, source parameters q_p^0, q_{He}^0, α_p and α_{He} are automatically adjusted to find the best fit for both proton and helium data.

Table 1 The sets of cosmic ray injection and propagation parameters and the goodness of fit for different models considered in this paper. Models Aa (axisymmetric) and A (spiral) models assume point sources and instantaneous injection, while models B, C, D and E include effects of finite size and escape index. The index γ specifies the energy-dependence of the escape time (see Eq. (9)).

Model	A	Aa	B	C	D	E
Diffusion coefficient normalization K_0	0.0112	0.0112	0.0112	0.0112	0.0112	0.0112
Diffusion spectral index δ	0.7	0.7	0.7	0.7	0.7	0.7
Magnetic halo half thickness L [kpc]	4	4	4	4	4	4
Convective velocity V_c [km s^{-1}]	12	12	12	12	12	12
SN explosion rate ν [century^{-1}]	0.8	0.8	1.2	1.4	1.7	1.5
SN proton injection number q_p^0 [10^{52} GeV^{-1}]	2.527	1.773	1.355	1.188	0.933	1.068
SN proton spectral index α_p	2.2	2.17	2.154	2.159	2.150	2.151
SN helium injection number q_{He}^0 [10^{51} GeV^{-1}]	1.475	1.044	0.768	0.734	0.554	0.648
SN helium spectral index α_{He}	2.07	2.04	2.012	2.037	2.017	2.024
escape index	∞	∞	2	3	2.36	2.37
Goodness of fit $\chi^2/$dof	2.19	1.93	1.708	1.552	1.751	1.469

First, we study the spiral distribution model with instantaneous injection for local sources (model A). The average supernova explosion rate is taken as 0.8 per century. The results are presented in Figure 2, where the upper curves are for proton and lower curves for helium. The contribution from background sources Φ_{ext} is plotted as the green dashed lines, the contribution from nearby young sources Φ_{cat} as the purple dash-dotted lines and the total flux as the blue solid lines. The background flux Φ_{ext} is dominant below ~ 100 GeV, where the AMS-02 data dominate the fit. As energy increases, the background contribution shrinks, while the contribution from nearby young sources increases.

As shown in Table 1, we find that compared with the original axisymmetric model (Bernard et al. 2013), the goodness of fit for the spiral model is not improved. To understand this, in Figure 3 we compare the proton flux for models A (spiral) and Aa (axisymmetric). Both models are based on the same cosmic ray propagation parameters, and have the same average supernova explosion rate ν. The solid curves correspond to the spiral model A whereas the dashed curves feature the axisymmetric model Aa. For the low energy part, the two models have almost the same background contribution. Now that the Earth is located between the Carina–Sagittarius and Perseus arms, the number of sources which contribute to Φ_{ext} are less numerous in the spiral model than for the axisymmetric model. The latter tends to overpopulate the void inside which the solar system is located and leads to a slightly larger background flux above ~ 1 TeV. This effect is counterbalanced by a smaller contribution Φ_{cat} from the local sources up to an energy of 10 TeV, so the best-fit value for q_p^0 is larger in model A than in model Aa. Conversely, the high-energy data points demand a slightly softer injection spectrum and a larger value for the index α_p in model A than Aa. However, the difference between model A and model Aa is not very significant. Perhaps more important is the behavior of the background flux Φ_{ext} at high energy in the presence of spiral arms; as the energy increases, it drops faster than the simple power law as was assumed in Thoudam & Hörandel (2012, 2013b).

Next, we consider the energy-dependent injection from local sources; the background sources are assumed to be spirally distributed. As we discussed earlier, modifying the escape index γ changes the energy range where the local component comes into play. When γ becomes large, the energy-dependent escape gradually approaches an instantaneous injection taking place at the start of the Sedov phase, and sources then behave as point-like objects (the radius is only ~ 5 pc). As γ decreases, the span of the escape time becomes longer. The most energetic particles escape first from the SNR. When the injection timescale becomes comparable with the upper limit of $30\,000$ yr for the age of local sources, only the most energetic cosmic rays are released and make it to Earth. We
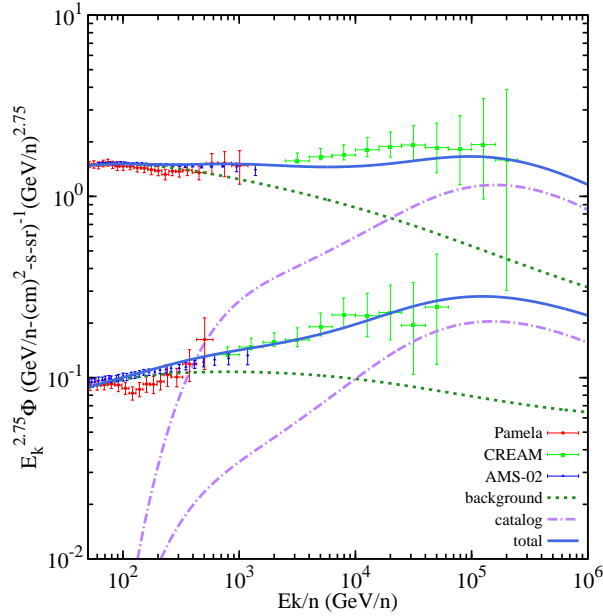
Fig. 2 The best-fit model A (see Table 1) to the AMS-02 and CREAM data under the case of spiral distribution of background sources, where local sources are assumed to be point-like with instantaneous injection. The propagation parameters are configured to the MED case, where L is 4 kpc, and an explosion rate of 0.8 per century is assumed. Proton (*upper curves*) and helium (*lower curves*) spectra are featured in the energy range extending from 50 GeV/nuc to 100 TeV/nuc. The contribution from the background sources corresponds to the green dashed lines. The blue solid lines show the total flux while the purple dash-dotted curves indicate the flux from the sources of the catalog.

explored different values of γ and found that at γ values of $2 \sim 3$, good fits can be obtained. In the best-fit models B and C, the MED propagation parameters are assumed, with $\gamma = 2$ and $\gamma = 3$ for models B and C, respectively. Here, we explore how the local flux Φ_{cat} reacts to a change in the escape index γ.

The results are shown in Figures 4 and 5. There is a low energy cut-off in the local contributions to the proton and helium fluxes in the case of model B where $\gamma = 2$ has been assumed. This is due to the energy-dependent cosmic ray release mechanism we discussed earlier; the lower energy cosmic ray particles from young sources have not yet been released or reached Earth. As a result of this low energy cut-off, there is also a kink at this energy in the spectrum predicted by the model. In model C, with $\gamma = 3$, the cutoff is not as sharp and the local flux starts to contribute to lower energies. The kink in total flux at low energy in model B (Fig. 4) disappears in model C (Fig. 5).

We find that, when taking the energy-dependent escape into account, the goodness of fit is markedly improved. For completeness, we have also varied the supernova explosion rate between models B and C. A larger value of ν translates into a larger abundance of sources contributing to the overall signal. The amount of cosmic rays injected by a single object decreases, as is clearly shown in Table 1. Although the effect is marginal, the contribution from local sources drops gradually when increasing the explosion rate.

Finally, we consider the injection index γ to be a free parameter and let it vary between 2 and 3. Model D (Fig. 6) and model E (Fig. 7) are for SN explosion rates of 1.7 and 1.5 per century, respec-
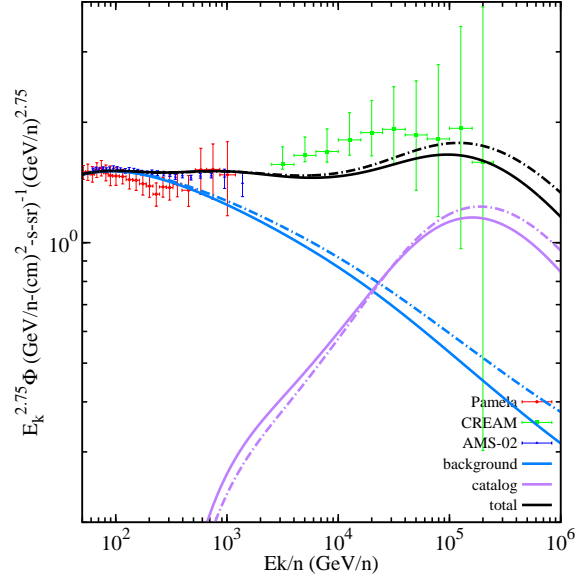
Fig. 3 Various contributions to the proton flux have been calculated in the spiral and axisymmetric source models for the purpose of comparison. The solid and dashed correspond to the spiral and axisymmetric configurations A and Aa of Table 1 respectively. The black lines feature the total flux, which is a sum of the contributions from the background sources (*blue*) and from the catalog of local objects (*purple*).
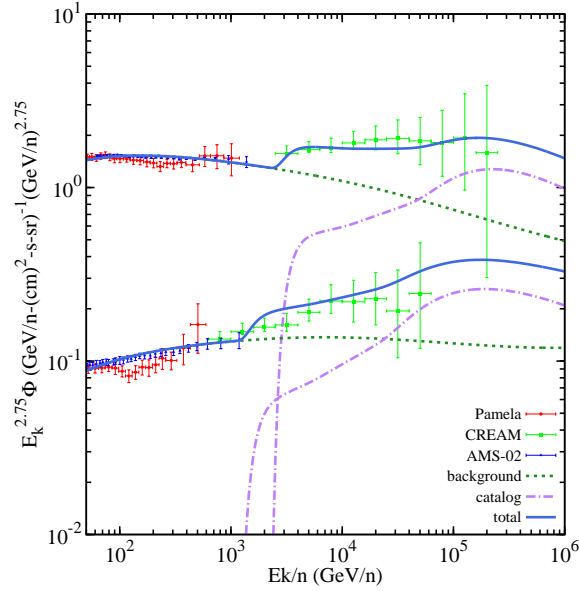

Fig. 4 Model B assumes an energy-dependent escape of cosmic rays from local sources. The escape index γ is set equal to 2 as a default value, while the explosion rate is equal to 1.2 per century. The cosmic ray propagation parameters are configured to the MED model.
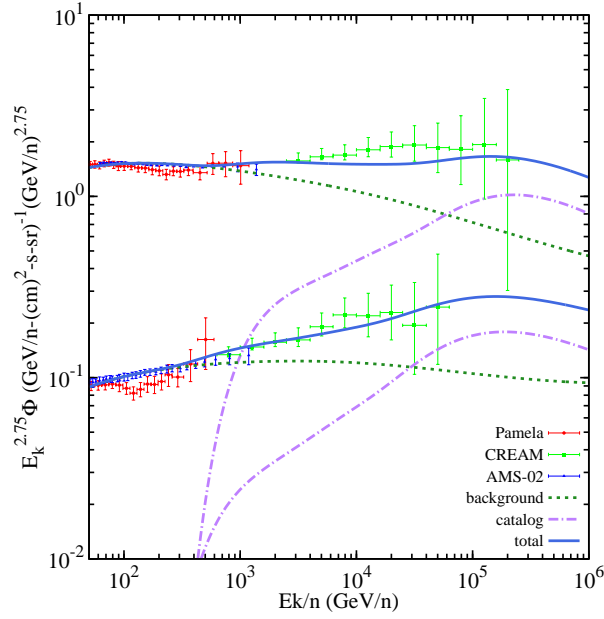
Fig. 5 Another best-fit model C with the same constraints as before. The escape index γ is set equal to 3 as a default value and the explosion rate is equal to 1.4 per century.
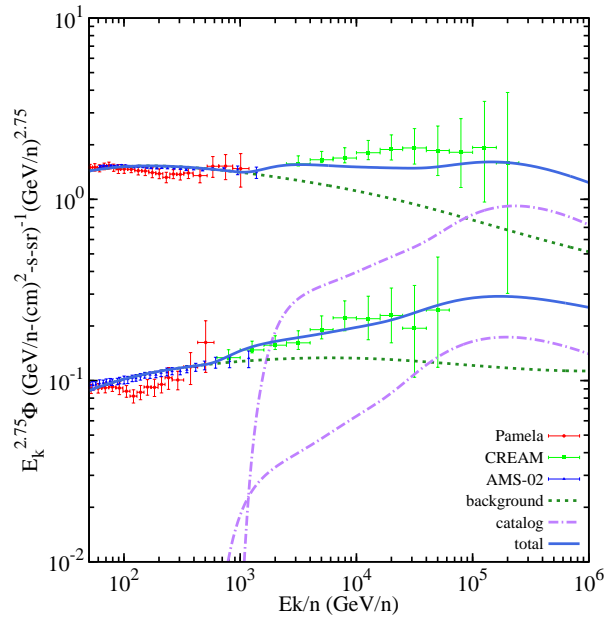

Fig. 6 The best-fit model D is obtained by setting the explosion rate ν equal to 1.7 per century and by letting the escape index γ vary between 2 and 3. The latter adjusts itself to a value of 2.36, close to 2, hence there is a kink in the proton and helium spectra at ~ 1 TeV/nuc.
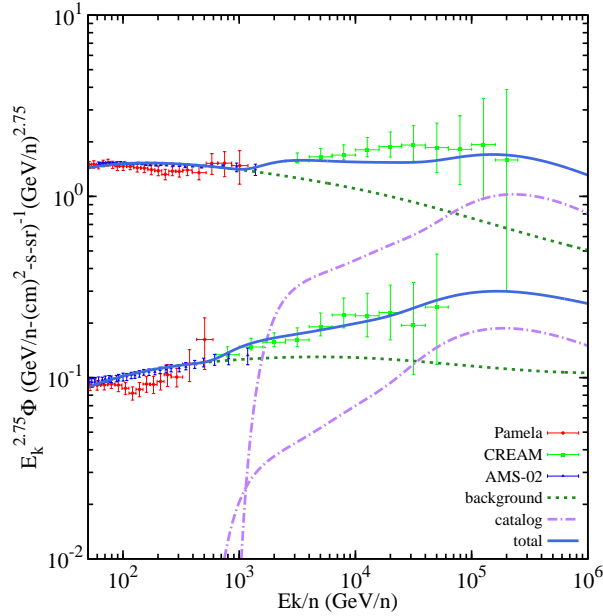
Fig. 7 The previous fit is improved in model E, where the explosion rate ν is now decreased to a value of 1.5 per century.

tively. These values are very close to the average determined by Diehl et al. (2006). Furthermore, increasing the explosion rate would make the fitting worse, especially for the proton spectrum.

5 CONCLUSIONS

The spectral hardening exhibited by the cosmic ray proton and helium fluxes above a few hundred GeV/nuc in the PAMELA (Adriani et al. 2011) data is no longer present in the AMS-02 (AMS-02 2013) observations, which point toward a power law behavior. However, the CREAM (Ahn et al. 2010; Yoon et al. 2011) experiment still reports an excess above ~ 1 TeV/nuc, which is hard to understand in the conventional model of cosmic ray transport, and the problem persists. Here, we propose a solution in terms of the known local and young SNRs whose contributions become dominant above TeV energies. These sources have been extracted from astronomical catalogs. The cosmic ray transport model has also been set to the MED configuration best fits the B/C ratio. The thickness of the diffusive halo is 4 kpc, a value that has been so far considered as canonical.

In this paper, we have improved over our previous analysis in three respects. To commence, we have used the AMS-02 data which are much more difficult to accommodate with a TeV spectral hardening than the PAMELA observations. The goodness of our fits suffers from the power law behavior of the AMS-02 measurements as well as from smaller error bars associated with a significant improvement in the accuracy of the data. In spite of this, we get reduced chi-square values which are still satisfactory. To do so, we have introduced two major revisions for the sources of our model. Supernova explosions are distributed along spiral arms as they should be in a typical SBc galaxy such as the Milky Way. The previous axisymmetric distribution of cosmic ray background sources has thus been replaced by a spiral distribution. Then, we have explicitly taken into account the finite size of the local sources, for which this effect is the most severe, and we have also modeled the energy-dependent escape of cosmic rays from them.

We find that considering a spiral distribution for the cosmic ray background sources only leads to limited improvements. By contrast, a better description of local sources induces obvious effects. For the canonical MED model of cosmic ray transport parameters, the average explosion rate ν can be as large as 1.5 per century, or even 1.7 for model D, and becomes close to the fiducial value of 1.9 ± 1.1 found by Diehl et al. (2006). This is a significant improvement over the Bernard et al. (2013) analysis, where ν had to be as small as 0.8 per century, with a reduced chi-square value of 1.3 based on the PAMELA data, to be compared to our best-fit result of 1.47 obtained with the more constrained AMS-02 measurements. We confirm that a higher explosion rate reduces the role of local sources, as is clear in Table 1, where the proton and helium yields of q_p^0 and q_{He}^0 are anticorrelated with ν. Our best-fit models D and E feature a characteristic kink at a few TeV/nuc. Should this hardening be confirmed by future observations, it would point toward sources where the release of cosmic rays in interstellar space cannot be considered as instantaneous, with the most energetic particles being emitted first.

References

Adriani, O., Barbarino, G. C., Bazilevskaya, G. A., et al. 2011, Science, 332, 69

Ahn, H. S., Allison, P., Bagliesi, M. G., et al. 2010, ApJ, 714, L89

Amenomori, M., Bi, X. J., Chen, D., et al. 2011, Astrophysics and Space Sciences Transactions, 7, 15

AMS-02 2013, *http://www.ams02.org/*

Ave, M., Boyle, P. J., Höppner, C., Marshall, J., & Müller, D. 2009, ApJ, 697, 106

Axford, W. I., Leer, E., & Skadron, G. 1977, International Cosmic Ray Conference, 11, 132

Bell, A. R. 1978, MNRAS, 182, 147

Berezinskii, V. S., Bulanov, S. V., Dogiel, V. A., & Ptuskin, V. S. 1990, Astrophysics of Cosmic Rays, ed. Ginzburg, V. L. (Amsterdam: North-Holland)

Bernard, G., Delahaye, T., Keum, Y.-Y., et al. 2013, A&A, 555, A48

Bernard, G., Delahaye, T., Salati, P., & Taillet, R. 2012, A&A, 544, A92

Biermann, P. L., Becker, J. K., Dreyer, J., et al. 2010, ApJ, 725, 184

Blandford, R. D., & Ostriker, J. P. 1978, ApJ, 221, L29

Blasi, P., & Amato, E. 2012, J. Cosmol. Astropart. Phys., 1, 010

Blasi, P., Amato, E., & Serpico, P. D. 2012, Physical Review Letters, 109, 061101

Bringmann, T., Donato, F., & Lineros, R. A. 2012, J. Cosmol. Astropart. Phys., 1, 049

Consolandi, C., & on Behalf of the AMS-02 Collaboration 2014, arXiv:1402.0467

Di Bernardo, G., Evoli, C., Gaggero, D., Grasso, D., & Maccione, L. 2010, Astroparticle Physics, 34, 274

Di Bernardo, G., Evoli, C., Gaggero, D., Grasso, D., & Maccione, L. 2013, J. Cosmol. Astropart. Phys., 3, 036

Diehl, R., Halloin, H., Kretschmer, K., et al. 2006, Nature, 439, 45

Donato, F., Fornengo, N., Maurin, D., Salati, P., & Taillet, R. 2004, Phys. Rev. D, 69, 063501

Effenberger, F., Fichtner, H., Scherer, K., & Büsching, I. 2012, arXiv:1210.1423

Elmegreen, D. M. 1998, Galaxies and Galactic Structure (New Jersey: Prentice Hall)

Erlykin, A. D., & Wolfendale, A. W. 2012, Astroparticle Physics, 35, 371

Evoli, C., Gaggero, D., Grasso, D., & Maccione, L. 2008, J. Cosmol. Astropart. Phys., 10, 018

Faucher-Giguère, C.-A., & Kaspi, V. M. 2006, ApJ, 643, 332

Gaggero, D., Maccione, L., Di Bernardo, G., Evoli, C., & Grasso, D. 2013, Physical Review Letters, 111, 021102

Green, D. A. 2009, Bulletin of the Astronomical Society of India, 37, 45

Higdon, J. C., & Lingenfelter, R. E. 2003, ApJ, 582, 330

Krymskii, G. F. 1977, Akademiia Nauk SSSR Doklady, 234, 1306

Malkov, M. A., Diamond, P. H., & Sagdeev, R. Z. 2012, Physical Review Letters, 108, 081104

Manchester, R. N., Hobbs, G. B., Teoh, A., & Hobbs, M. 2005, AJ, 129, 1993

Maurin, D., Donato, F., Taillet, R., & Salati, P. 2001, ApJ, 555, 585

Maurin, D., Taillet, R., & Donato, F. 2002a, A&A, 394, 1039

Maurin, D., Taillet, R., Donato, F., et al. 2002b, arXiv:astro-ph/0212111

Nakamura, K., & Particle Data Group 2010, Journal of Physics G Nuclear Physics, 37, 075021

Norbury, J. W., & Townsend, L. W. 2007, Nuclear Instruments and Methods in Physics Research Section B: Beam Interactions with Materials and Atoms, 254, 187

Ohira, Y., & Ioka, K. 2011, ApJ, 729, L13

Shaviv, N. J. 2002, Physical Review Letters, 89, 051102

Shaviv, N. J. 2003, New Astron., 8, 39

Shaviv, N. J., Nakar, E., & Piran, T. 2009, Physical Review Letters, 103, 111302

Strong, A. W., & Moskalenko, I. V. 1998, ApJ, 509, 212

Strong, A. W., Moskalenko, I. V., & Ptuskin, V. S. 2007, Annual Review of Nuclear and Particle Science, 57, 285

Strong, A. W., Porter, T. A., Digel, S. W., et al. 2010, ApJ, 722, L58

Thoudam, S., & Hörandel, J. R. 2012, MNRAS, 421, 1209

Thoudam, S., & Hörandel, J. R. 2013a, arXiv:1308.1357

Thoudam, S., & Hörandel, J. R. 2013b, arXiv:1304.1400

Tibet Asγ Collaboration, Amenomori, M., Bi, X. J., et al. 2011, Advances in Space Research, 47, 629

Tomassetti, N. 2012, ApJ, 752, L13

Vallee, J. P. 1995, ApJ, 454, 119

Vallée, J. P. 2002, ApJ, 566, 261

Vladimirov, A. E., Jóhannesson, G., Moskalenko, I. V., & Porter, T. A. 2012, ApJ, 752, 68

Yoon, Y. S., Ahn, H. S., Allison, P. S., et al. 2011, ApJ, 728, 122

Yuan, Q., Zhang, B., & Bi, X.-J. 2011, Phys. Rev. D, 84, 043002

Yusifov, I., & Küçük, I. 2004, A&A, 422, 545